

## Performance Evaluation of a Solar Assisted Dual Condenser Heat Pump System for Drying of Pandan Leaves (*Pandanus Amaryllifolius*)

Rohaimi Abdullah<sup>a,b</sup>, Adnan Ibrahim<sup>a\*</sup>, Muhammad Amir Aziat Bin Ishak<sup>c</sup>, Kamaruzzaman Sopian<sup>d</sup>, Hasila Jarimi<sup>a</sup>, Halim Razali<sup>a</sup> & Ghaith Abusaibaa<sup>a</sup>

<sup>a</sup>*Solar Energy Research Institute, Universiti Kebangsaan Malaysia, 43600, Selangor, Malaysia,*

<sup>b</sup>*Section of HVAC&R, Universiti Kuala Lumpur Malaysia France Institute, 43650 Bandar Baru Bangi, Selangor Malaysia*

<sup>c</sup>*Faculty of Innovation & Technology, Taylor's University Lakeside Campus, 47500 Subang Jaya, Selangor*

<sup>d</sup>*Department of Mechanical Engineering, Universiti Teknologi PETRONAS, 32610Sri Iskandar, Perak Darul Ridzuan, Malaysia*

\*Corresponding author: [iadnan@ukm.edu.my](mailto:iadnan@ukm.edu.my)

Received 23 August 2024, Received in revised form 24 October 2024

Accepted 24 November 2024, Available online 30 January 2025

### ABSTRACT

The solar-assisted heat pump drying (SAHPD) system uniquely incorporates solar-heating refrigerant through hot water from solar evacuated tubes, offering distinct advantages. This study analyzed three experimental setups: a heat pump dryer (HPD) without solar assistance, SAHPD configuration 1 (C1-SAHPD) with solar-heated refrigerant at the discharge line, and SAHPD configuration 2 (C2-SAHPD) with solar-heated refrigerant between condensers, both for performance and economic viability. The experiments maintained consistent parameters, including 5.5 kg of Pandan leaf (*Pandanus amaryllifolius*), an airflow rate of 0.135 kg/s, and a refrigerant operating pressure of 9.65 bar. The SAHPDs operated when the hot water temperature in the storage tank reached between 70°C and 90°C, with a daily average radiation intensity ranging from 0.670 to 1.102 kW/m<sup>2</sup> for heating the water. The study revealed average coefficients of performance (COP<sub>avg</sub>) of 5.34, 5.43, and 6.53 for HPD, C1-SAHPD, and C2-SAHPD, respectively. The specific moisture extraction rate (SMER) for HPD was 2.64, while C1-SAHPD and C2-SAHPD had SMERs of 1.88 and 2.71 at solar fractions of 0.34 and 0.45, respectively. Notably, C2-SAHPD reduced electricity consumption by 46%. The payback period for drying 11 kg of Pandan leaves per day was 4.56 months for HPD, 4.32 months for C1-SAHPD, and 3.84 months for C2-SAHPD. The study concluded that C2-SAHPD was the most efficient dryer system for Pandan leaves based on its higher efficiency, SMER, and cost recovery. Additionally, the performance optimization presented in this study contributed to developing a novel technique for classifying dryer technologies.

**Keywords:** Solar assisted heat pump dryer; solar-heating refrigerant; R32; COP; dual condenser; evacuated tube

### INTRODUCTION

A solar-assisted heat pump dryer (SAHPD) integrates solar thermal energy with a heat pump to form a hybrid heating system. Unlike an open heat pump dryer (HPD), a closed HPD does not absorb heat from external air or other sources (Assadeg et al. 2020). Consequently, the SAHPD enhances a closed-type heat pump, which otherwise suffers from insufficient heat due to its closed design (Yang, Zhu, &

Zhu 2013). The system can generate additional thermal energy by incorporating solar thermal energy (Reddy, 2008). The heat collected from sunlight is influenced by solar irradiation, heat transfer medium, and the type of collector used. Although solar energy is available only during daylight hours, some can be stored as hot water for night use. Thus, hybrid solar heating effectively boosts productivity while curbing fossil fuel energy consumption and reducing CO<sub>2</sub> emissions ((Ochs, Magni, & Dermentzidis 2022).

Integrating solar radiation into an air conditioning system, often referred to as solar or booster air conditioner, is a method that emerged about two decades ago. This method aims to provide cooling or heating effects by harnessing thermal energy from renewable sources, particularly sunlight. According to (Meunier Francis 2013), since 2010, new solutions have been introduced to the market that utilizes solar energy to perform certain thermal steps in the compression process of conventional cooling systems, which previously depended solely on mechanical compression. This technology enables the compressor capacity to be reduced in design, requiring less energy and refrigerant while maintaining overall system capacity.

Assadeg et al. reported that a solar-assisted heat pump dryer (SAHPD) is formed by integrating solar thermal energy into the heat pump dryer (HPD) through various heat collectors, such as solar thermal collectors, solar chimney systems, solar PV collectors, and solar PV/T collectors. There are two types of solar thermal collectors: liquid collectors and air collectors. This study proposes an SAHPD that employs a liquid-type solar thermal collector, which is more efficient than air collectors. Another reviewed paper discussed the benefits and drawbacks of flat-plate solar drying. One advantage of this type of solar dryer is its capability to treat materials in a clean atmosphere. However, drawbacks include the need for an effective control technique and the low density of solar radiation, necessitating a large energy collector surface. Combining a solar dryer with a heat pump can address some challenges while meeting the significant demand for industrial drying. Heat pumps can extract heat from the surrounding air or hot water from the ground (Daghigh, Ruslan, Sulaiman, & Sopian 2010).

Ahmed Khouya employed a heat pump and a concentrated photovoltaic thermal system (CPV/T) to power a heat pump dryer (HPD) in the wood drying process. The system's coefficient of performance (COP) ranged from 3.91 to 7.2, leading to an 86% reduction in energy consumption. Lowering the temperature from 75 °C to 65°C improved COP (Khouya 2020). The water-air-heated system utilizes an 11.5 kW compressor to generate heat from a condenser and elevating the water temperature to the desired level for drying. Singh and Gaur (2020) investigated heat transmission on a novel hybrid active greenhouse solar dryer (HAGSD) with a water-type transfer collector in a tube. Tomatoes, ginger, and bottle gourd dry faster in the dryer with evacuated tube collector (ETC) than in the dryer without ETC, with drying times of 9, 12, and 6 hours, respectively. The overall drying efficiency for the three crops ranged from 14.22 to 27.99% for the ETC dryer and 9.63 to 24.88% for the non-ETC dryer (Singh & Gaur 2020).

Maintaining the drying temperature is critical to preserving the quality of herbs, including their colour, total chlorophyll content, moisture content, and fibre content. The addition of 2.5% pandan leaf powder, dried in a cabinet drier at 40°C for 6 hours, yielded the optimal physical and organoleptic results, with brightness increasing at higher drying temperatures (Murtini, Yuwono, Setyawan, & Nadzifah 2020). Zou et al. noted that standard solar-assisted heat pump (SAHP) systems currently operate inefficiently at low ambient temperatures due to a mismatch between heat demand and SAHP heat supply. Thus, employing a modified heat pump cycle is crucial for enhancing drying efficiency (Abusaibaa, Sopian, Abdullah, Jarimi, & Ibrahim, 2022). Additionally, the heat pump drier uses solar energy, captured by solar collectors and delivered to either air or refrigerant, to heat and dry agricultural and marine materials (Hawladar & Jahangeer 2006). In this study, the evacuated tube collector (ETC) absorbs heat from the sun, heats the water circulating through it, and stores the heated water in a tank. The heated water in the tank then flows through a heat exchanger to heat the refrigerant.

A review report indicated that SAHPD technology enhances an HPD's temperature and drying rate. The SAHPD also offers benefits such as producing high-quality dried products, environmental protection, and energy efficiency. Previous SAHPD systems employed various methods of solar heat addition, including an attached hot water coil at an evaporator (Figure 4; Ismail et al.), an evaporator and collector (Figure 5), an attached hot water coil at a condenser (Figure 6), CPV/T and condenser-heated water (Figure 7), a PV/T evaporator (Figure 8), and suction heating (Figure 15) (Zou, Liu, Yu & Yu 2023). Unlike these previous methods, this paper details a novel approach to refrigerant heating at a dual condenser.

The literature presents numerous strategies in SAHPD to enhance the coefficient of performance (COP) using conventional setups. This study employs SAHPD to heat refrigerant at the discharge line and between condensers using solar thermal energy. Additionally, this study evaluates the viability of the novel SAHPD for herb drying through experimental testing in Malaysia's hot and humid climate. This unique system, the first of its kind, incorporates additional heat using a refrigerant heating method via hot water from a solar evacuated tube into the HPD with a dual condenser for herb drying. The key contribution of this study is the investigation of a solar drying system known as a 'solar-assisted heat pump', which utilizes two configurations of refrigerant heating methods with a dual condenser. Specifically, configuration 1 involves solar heating of the refrigerant at the discharge line, while configuration 2 involves solar heating of the refrigerant between the condensers. The performance of both configurations, namely C1-SAHPD and C2-SAHPD,

was evaluated and assessed. The practical analysis results reported for the three experimental settings, which included conventional HPD, C1-SAHPD, and C2-SAHPD, indicate a total heat demand of 11.545 MJ for drying 5.5 kg of

Pandan leaf (*Pandanus amaryllifolius*). The daily average radiation intensity for heating water ranged between 0.670 and 1.102 kW/m<sup>2</sup> (Din et al. 2024). Consequently, the SAHPDs operated when the hot water temperature in a storage tank reached 70 to 90°C.

### Nomenclature

a	Ambient	P	Work (W)
Am	Ante Meridiem	Pm	Post meridiem
avg	Average	PV	Photovoltaic
C	Configuration	Q	Heat energy (W)
COP	Coefficient of performance	Q <sub>s</sub>	Sensible energy (kW)
C <sub>p</sub>	Specific heat (kJ/kg.K)	q <sub>v</sub>	Volume flow rate (m <sup>3</sup> /s)
ch	Chamber	RH	Relative humidity
CO <sub>2</sub>	Carbon dioxide	R-32	Difluoro methylene (CH <sub>2</sub> F <sub>2</sub> )
dB	Dry bulb (°C)	Ref.	Refrigerant
E	Energy (W)	SMER	Specific moisture extraction rate
ETC	Evacuated tube collector	SSH	Suction superheat
HE	Heat exchanger	SC	Subcooling
h <sub>ig</sub>	Specific enthalpy (kJ/kg)	t	Time
K	Kelvin	TC	Thermocouple sensor
m	Mass (kg)	T	Temperature
MER	Moisture extraction rate	USD	US dollar
η	Efficiency	w	Water
ρ	Density (kg/m <sup>3</sup> )	wB	Wet bulb (°C)

TABLE 1. Meteorological data at SERI UKM, Bandar Baru Bangi, Malaysia (weather station)

	Oct-23	Nov-23	Dec-23	Jan-24	Feb-24	March-24
Average ambient temperature (°C)	29.6	28.8	28.1	29.4	30.4	30.4
Average daily total irradiation of the collector (MJ/m <sup>2</sup> .d)	15.48	14.38	14.30	15.59	15.65	15.79
Number of days (d)	31	30	31	31	29	31

## MATERIAL AND METHODS

The solar-assisted heat pump dryer (SAHPD) was installed and tested in the Solar Thermal Research Laboratory at Solar Energy Research Institute (SERI) of Universiti Kebangsaan Malaysia (UKM) in Bandar Baru Bangi, Malaysia (longitude 101.78°E, latitude 2.92°N). Meteorological data collected from the weather station are presented in Table 1. The research aimed to dry 5.5 kilograms of pandan leaves, which have a moisture content of 84.32%, as reported by E.S. Murtini et al. The experiment used the same amount of pandan leaves for HPD and SAHPD tests. The pandan leaves were separated and evenly distributed on ten fine wire netting-covered trays, each

measuring 1.495 m in length, 0.997 m in width, and 0.038 m in depth. Before drying, the fresh pandan leaves were chopped to approximately 0.1 m in length and manually placed in the trays. The drying process commenced with an initial weight of 5.5 kg and a moisture content of 5.4 g water/g matter (dry basis), which was reduced to 0.34 g water/g dried matter. The testing was concluded when the drying chamber's relative humidity (RH) decreased to approximately 25 to 21% RH. The dried pandan leaves from each tray were weighed using a digital scale (Kern FCE 3K1N).

This approach was consistently applied to all tests, including those for HPD and SAHPD systems.

## SYSTEM DESCRIPTION

Figure 1 illustrates the schematic of the overall SAHPD system used in the current investigation. The heat pump device in the SAHPD system comprises a compressor (inverter), a dual condenser with two fans, a fan coil, an electronic expansion valve (EEV), and an evaporator unit, all housed within a dryer cabinet compartment. The system includes 30 evacuated tube solar collectors outside the chamber facility, a heat storage tank, two circulation pumps, a plate-type heat exchanger, valves, and other components. Two identical condenser coils, each with its fan motor, are connected in series. R-32 refrigerant in the heat pump absorbs heat for evaporation, which is rejected at the first and second condensers after compression in the compressor. The heat rejected by the condenser is utilized to heat space dryers via the evaporator fan unit. The refrigerant cycle is completed by expanding the electronic expansion valve before entering the evaporator at a temperature of 6-15°C. Two axial fans and an evaporator fan flow hot air from the condenser (47-53°C) into the drying cabinet. The refrigerant then enters the evaporator, which absorbs heat and condenses moisture at the evaporator. The discharge line is connected to the heat exchanger, and the heat exchanger's outlet is connected to the condenser inlet.

At the onset of the closed-type drying process, a compressor and a limited amount of air within the dryer cabinet generate some initial heat. When fresh products are placed on trays in the drying chamber, they start to produce heat through respiration. The three heat sources – compressor, air, and respiration- combine in the circulated air to heat both the products and the trays. With the closed type of HPD, as depicted in Figure 1, the drying process requires some time to heat the air, resulting in a delayed attainment of the desired drying temperature.

Before the SAHPD becomes operational, 30 evacuated tubes are involved, with 15 tubes connected to each of the two manifolds linked in series to absorb solar heat. When the heat pipes within the evacuated tubes heat up, pump 1 circulates water in and out of the manifolds. Subsequently, hot water flows in and out of a storage tank at a flow rate of 0.2 kg/s. The water temperature in the tank gradually increases, and an auxiliary heater is used to raise the hot water temperature to 90°C, the maximum temperature of the tank, for testing purposes.

When the SAHPD is in operation, pump 2 circulates hot water from the tank through a heat exchanger (HE), transferring heat to the refrigerant. The heated refrigerant

then flows into the condenser, increasing its temperature and dehumidifying the air passing through it. This heating mechanism is referred to as solar-heating refrigerant. The solar-heating refrigerant method employs two configurations, C1-SAHPD and C2-SAHPD, as shown in Figures 2(a) and 2(b), respectively. Table 2 outlines the key system components, specifications, and characteristics, while Table 3 presents the characteristics of the various instruments used in the experiments. The hot water, heated by a solar collector, flows from the tank to the heat exchanger at a rate of 0.334 m<sup>3</sup>/s, causing the temperature of the discharge or liquid (outlet condenser 1) surface pipe to rise in accordance with the test hot water temperature, which ranges from 70°C to 90°C. Consequently, the chamber temperature and drying rate are predicted to increase steadily, along with the system's coefficient of performance (COP). Increasing the refrigerant superheat level out of the evaporator enhances the COP by approximately 0.1 to 0.23% for each 1K rise in superheat degree (Ardita, Wirajati, & Sudirman, 2020). When using C1-SAHPD, three (3) of V1 should be open and four (4) of V2 should be closed; conversely, for C2-SAHPD, three (3) of V1 should be closed and four (4) V2 should be open, directing the refrigeration flow appropriately.

## THERMODYNAMIC ANALYSIS OF HPD AND SAHPD SYSTEMS

$$Q_t = Q_{SD} + Q_{HPD} \quad (1)$$

Where  $Q_t$  is the total heat energy required for the drying process (kJ),  $Q_{SD}$  is the solar system's heat (kJ), and  $Q_{HPD}$  is the heat generated by the HPD system (kJ). System heat balance equation (Qiu et al. 2016).

## THE LOAD NECESSARY HEAT FOR THE PROCESS OF DRYING

The necessary heat for the drying process includes the energy needed to heat the pandan leaves, the energy needed to evaporate water, and the heat lost during the drying process (Qiu et al.). The necessary heating heat to pandan leaves:

$$Q_p = C_r m i (T_{rf} - T_{ri}) \quad (2)$$

Where  $m_i$  is the Pandan leaves' initial mass (kg), and  $C_p$  is their specific heat at constant pressure (kJ/(kg°C)).  $T_{rf}$  represents the final temperature of pandan leaves.  $T_{ri}$  represents the initial temperature of Pandan leaves (°C). The required heat to evaporate water:

$$Q_e = \gamma \times (m_i - m_f) \tag{3}$$

Where  $m_i$  is the initial mass of Pandan leaves (kg),  $m_f$  is the final mass of Pandan leaves (kg), and  $\gamma$  represents the latent heat of vaporization (kJ/kg). The loss of thermal energy during the drying process:

$$Q_l = (Q_p + Q_e) \times 10\% \tag{4}$$

The total required heat during the drying process:

$$Q_t = Q_p + Q_e + Q_l \tag{5}$$

### THE HEAT GENERATED BY THE SOLAR DRYING SYSTEM

The amount of solar radiation captured by the collector during the testing can be expressed as follows:

$$G = 3.6 \int_0^t A_c I_t dt \tag{6}$$

where  $A_c$  is the collector area (m<sup>2</sup>), and  $I_t$  is the amount of solar energy incident on the collection (W/m<sup>2</sup>). The solar system's heat can be stated as follows:

$$Q_s = G \eta_s \eta_c \tag{7}$$

where  $G$  is the daily total solar radiation incident on the collector (kJ),  $\eta_c$  is the collector's efficiency, and  $\eta_s$  is the efficiency of transporting heat from the water storage tank.

The solar fraction (SF) can be calculated using Eq. 8:

$$SF = \frac{Q_s}{Q_t} \tag{8}$$

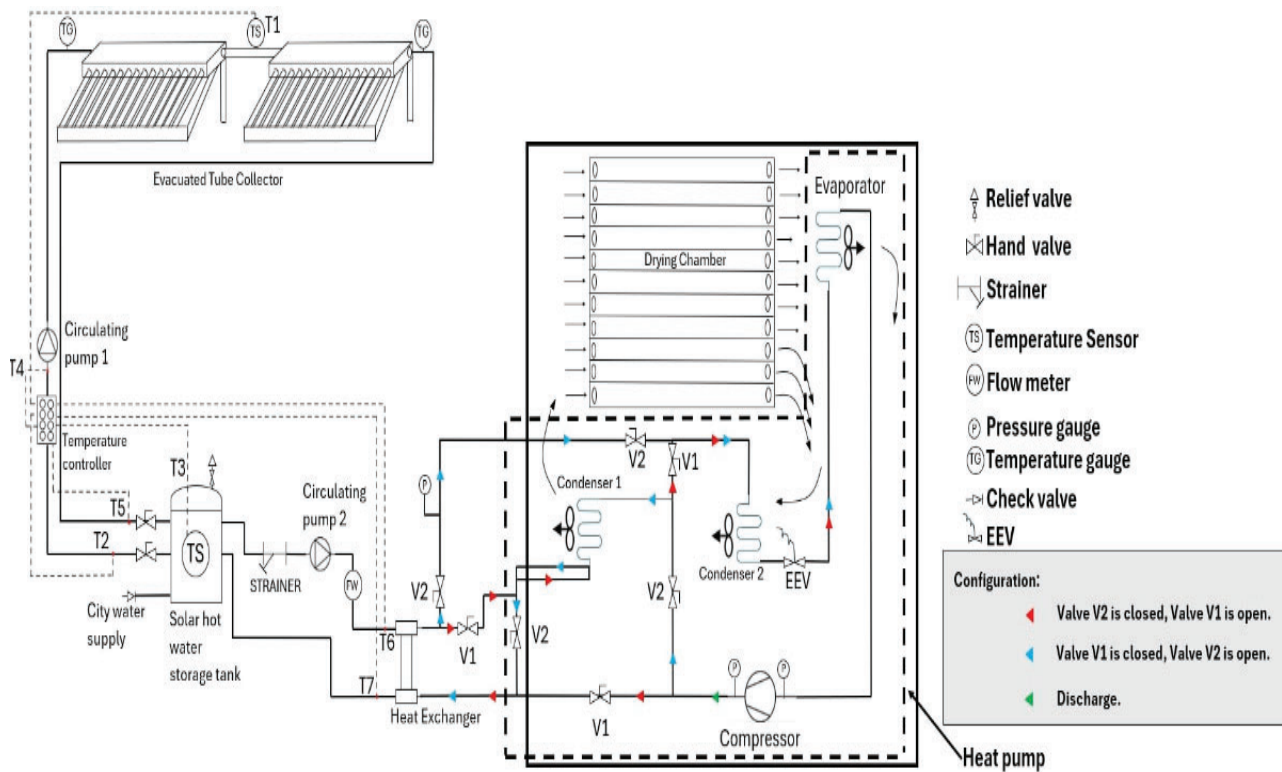


FIGURE 1. Solar Assisted Heat Pump Dryer (SAHPD) system

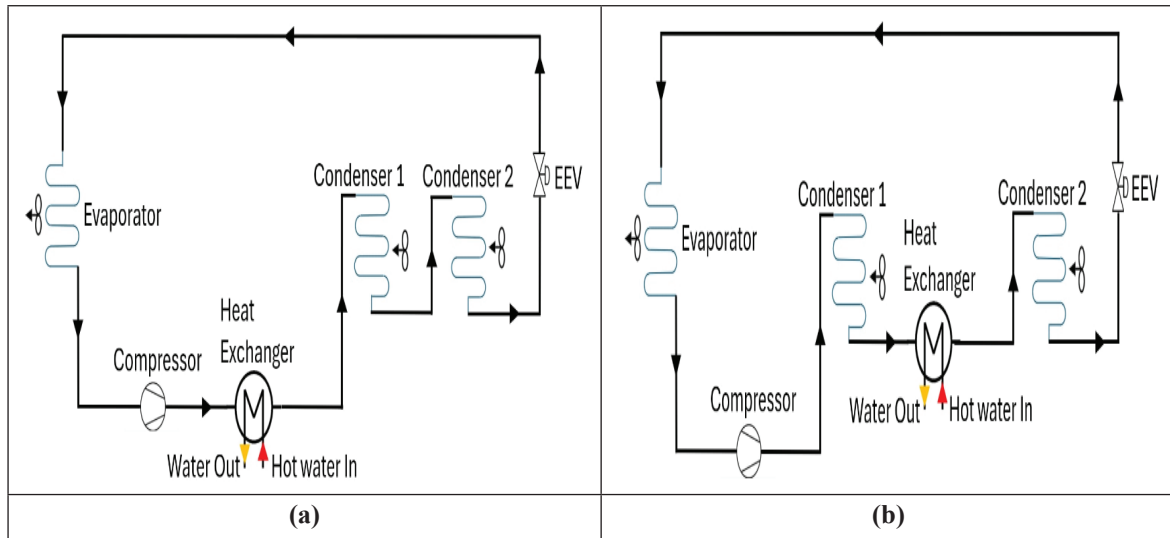


FIGURE 2. Schematic of SAHPDs a) solar-heating refrigerant at discharge line (C1-SAHPD), (b) solar-heating refrigerant between condensers (C2-SAHPD)

TABLE 2. The primary component specifications and the system parameter characteristics.

Item	Specification and characteristics
Collector's tilt angle	45°
Size of a glass tube	Ø58 mm x L1800 mm
Number of tubes	30
The surface area of the collector	5.58 m <sup>2</sup>
Surface area of absorber	9.75 m <sup>2</sup>
Collector's efficiency	Optical efficiency is 0.65; heat loss coefficient is 0.78 W/m <sup>2</sup> °C
Water storage tank	Volume: 300 liters (dm <sup>3</sup> )
Heat pump	Compressor rated power: 2 HP (1.5kW), rated cooling capacity 5.27kW, thermal output: 5.89kW
Circulating air fan	Rated power: 500 W

## THE PERFORMANCE EVALUATION OF THE SUBSYSTEM OF SOLAR DRYIN

The storage heat of the water storage tank can be stated as:

$$G_s = 3600 \int_0^t \dot{m}_w C_w (T_{wout} - T_{win}) dt \quad (9)$$

In Eq. 9,  $\dot{m}_w$  represents the water flow rate through the collector (kg/s),  $C_w$  is the specific heat of water at constant pressure (kJ/kg°C),  $T_{wout}$  is the water temperature at the collector's outlet (°C), and  $T_{win}$  is the water temperature at the collector's inlet (°C). Or (Chen, Wong, & Li, 2015):

$$= 3600 E_d A_c \eta_c \quad (10)$$

Where  $E_d$  is daily energy supply (kWh/m<sup>2</sup>day),  $A_c$  is the area of the solar collector (m<sup>2</sup>), and  $\eta_c$  is solar collector efficiency.

## THE HEAT FROM THE HEAT PUMP DRYING SYSTEM (HPD)

A condenser's thermal power is expressed as follows:

$$P_c = \dot{m}_a C_a (T_{aoutc} - T_{ainc}) \quad (11)$$

Where  $\dot{m}$  is the mass flow rate of air passing through the condenser (kg/s),  $C_a$  is the specific heat of the air (kJ/kg°C),  $T_{ainc}$  is the air temperature at the condenser inlet (°C), and  $T_{aoutc}$  is the air temperature at the condenser outlet (°C).

Therefore, the provided heat of the HPD system can be expressed as:

$$Q_{HPD} = \int_0^t P_c dt \quad (12)$$

### WITHOUT AN EVACUATED TUBE COLLECTOR

A Mollier chart (P-H diagram) is used to analyze the performance of the refrigeration system of the HPD. All data measured in the refrigeration system is plotted on the Mollier chart or input into Solkane software further to investigate the Coefficient of Performance (COP) value. The COP, an efficiency measurement, reflects the system's ability to remove moisture (drying) from the leaves; the higher COP indicates a more efficient system. Therefore, defining the system's efficiency without an evacuated tube solar collector is appropriate, as shown in Eq. 13 or Eq. 14.

$$COP = P_c \div P \quad (13)$$

$$\text{or COP} = (h_2 - h_4) \div (h_2 - h_1) \quad (14)$$

### THE HEAT FROM THE SOLAR-ASSISTED HEAT PUMP DRYING SYSTEM (SAHPD) WITH EVACUATED TUBE COLLECTOR

In this research, a solar evacuated tube collector (ETC) is assumed to be used with the heat pump. The useful energy gain  $Q_u$  and efficiency  $\eta$  for the ETC can be calculated using the following expressions (15),(16):

$$\eta = a_0 - a_1 \frac{(\Delta T)}{I_T} - a_2 \frac{(\Delta T)^2}{I_T} \quad (15)$$

$$Q_u = \dot{m}C_p(T_{out} - T_{in}) \quad (16)$$

Where  $a_0$  [-] is the Intercept (maximum) of the collector efficiency,  $a_1$  is [kJ/h-m<sup>2</sup>-K] Negative of the first-order coefficient in the collector efficiency equation,  $a_2$  [kJ/h-m<sup>2</sup>-K<sup>2</sup>] Negative of the second-order coefficient in collector efficiency equation,  $I_T$  [kJ/h-m<sup>2</sup>] Global radiation incident on the solar collector (Tilted surface).

### COEFFICIENT OF PERFORMANCE AND SOLAR FRACTION FOR DRYER HEATING

The Coefficient of Performance COP and Solar fraction SF for space of dryer heating SAHPD is defined as follows:

$$COP_{HP} = Q_{con} / W_{comp} \quad (17)$$

$$Q_{con} = \dot{m} * C_p * \Delta T \quad (18)$$

$$SF = Q_u / W_{comp} \quad (19)$$

### EFFECTIVENESS OF HEAT EXCHANGER

The effectiveness-NTU approach significantly simplifies heat exchanger analysis. The heat transfer efficacy ( $\epsilon$ ) is a dimensionless quantity used in this approach and is defined as Eq. 20 (Meunier, F., Rivet, P., 2005), (Kareem & AlHayes, 2018), (Abdullah, 2018).

$$Effectiveness(\epsilon) = (T_{wi} - T_{ro}) / (T_{wi} - T_{ri}) \quad (20)$$

### DRYING CHARACTERISTICS ANALYSIS OF MATERIALS

Materials placed in the drying chamber are dried by the hot air at above 50 °C. The rate of drying time, material quality, and energy consumption by this system have been recorded and observed. To calculate the drying rate of the drying system, the following equations are used:

$$M = \frac{m - m_d}{m_d} \quad (21)$$

where  $m$  and  $m_d$  denote the mass of the material (kg) and the mass of the associated dry matter (kg).

The rate of drying can be calculated as follows:

$$DR = \frac{dM}{dt} = \frac{M_{t+\Delta t} - M_t}{\Delta t} \quad (22)$$

$M_t$  and  $M_{t+\Delta t}$  represent moisture content at "t" and "t+  $\Delta t$ " (g moisture/g dry matter), respectively; "t" refers to drying time (h).

## UNCERTAINTY ANALYSIS

The systematic approach of uncertainty analysis identifies measurement flaws. Measurement inaccuracies raise concerns about the data's veracity. Table 3 presents the results of the uncertainty analysis for the each measuring equipment. The analysis demonstrated that high-grade measurements were precise and reliable, with an uncertainty of less than 2%. The overall measurement errors are calculated using the following Eq. 23 (E.L.Rulazi et al.):

$$w_{total} = \sqrt{w_{temperature}^2 + w_{solar}^2 + w_{scale}^2 + w_{velocity}^2 + w_{humidity}^2 + w_{pressure}^2} \quad (23)$$

## ECONOMIC ANALYSIS OF THE SYSTEM

### LIFE-CYCLE METHOD AND DRYING COST AND PROFITABILITY

The cumulative net present worth for the life of a dryer, or the life cycle saving for the dryer, as discussed by (Qiu et al.), and drying cost and profitability by (Boroze et al. 2014) is given in Eq. 24:

$$V_{cnp} = \sum_{t=1}^t V_{npt} \quad (24)$$

In Eq. 25, the  $V_{npt}$  is the present worth of a dryer in a period of time (t) by year, which can be calculated as:

$$V_{npt} = \frac{(1+i)^{t-1}}{(1+n)^t} \times S_d \times D \quad (25)$$

where  $i$  is the inflation rate,  $n$  is the long-term investment interest rate,  $D$  is the number of dryer days used per year, and  $S_d$  is the annual daily savings (USD/d) for a dryer over time (t), as provided by Eq. 26.

$$S_d = (C_s - C_{ds}) \times m_f \quad (26)$$

where  $C_s$  is the selling price of dried pandan (USD/kg), and Eq. 27 estimates the cost per kilogram of dried pandan for a dryer ( $C_{ds}$ ).

$$C_{ds} = C_{fd} + C_d \quad (27)$$

where  $C_{fd}$  is the cost of fresh pandan per kilogram of dried pandan (USD/kg), and  $C_d$  is the cost of drying per kilogram of dried pandan in a drier (USD/kg), which are computed using Eqs. 28 and 29, respectively.

$$C_{fd} = \frac{m_f}{m_i} C_f \quad (28)$$

Where  $C_f$  represents the cost per kilogram of fresh pandan (USD/kg).

$$C_d = \frac{C_a}{m_f \times D} \quad (29)$$

In Eq. 30, the  $C_a$  represents the annual cost of a dryer and may be computed as:

$$C_a = C_{ac} + C_m + C_r \quad (30)$$

where  $C_{ac}$  is a dryer's annual capital cost (USD), as calculated by Eq. 31,  $C_m$  is a dryer's annual maintenance cost (USD), and  $C_r$  is a dryer's annual operating cost (USD).

$$C_{ac} = C_{cc} \times \frac{n(1+n)^j}{(1+n)^j - 1} \quad (31)$$

Where  $C_{cc}$  is the dryer's capital cost (in USD), and  $j$  is its life (in years).

Eq. 32 calculates the annual running cost of the drying system in HPD mode.

$$C_r = \frac{m_f - m_i}{SMER_{hpd}} \times D_{hpd} \times C_e \quad (32)$$

Where  $C_e$  represents the cost per kWh of electricity (USD/kWh).

## PAYBACK PERIOD

Eq. 33 calculates the payback period (N).

$$N = \frac{\ln(1 - \frac{C_{cc}}{V_{npt}}(n-1))}{\ln(\frac{1+i}{1+n})} \quad (33)$$

TABLE 3. Instrument characteristics.

Instrument	Range	Accuracy
Digital balance	0 – 15 kg	0.001kg
Humidity sensors	1-99%	± 3%RH
Data logger (AT4808)	-200 °C to 350°C	± 0.1°C
Anemometer	0-10 m/s	± 0.05%
Pressure gauge (Refco)	0-41 bar	± 0.1%
Pyranometer	0-2000 W/m <sup>2</sup>	± 1.5 W/m <sup>2</sup>

## RESULT AND DISCUSSION

The coefficient of performance (COP) of the SAHPD, utilizing solar-heating refrigerant as a heat addition method into HPD, was investigated using two sets of experimental data with varying heat addition configurations in a refrigeration system. These configurations are referred to as C1-SAHPD (refrigerant heating at the discharge line) and C2-SAHPD (refrigerant heating between condensers). Solar irradiation was increased from 0.670 to 1.110 kW/m<sup>2</sup> to heat water via pump 1 at 0.2 kg/s through ETC, which was then circulated by pump 2 from the storage tank at a flow rate of 0.334m<sup>3</sup>/s to heat refrigerant in the heat exchanger (HE). The HE exhibited an effectiveness value of 0.59. The refrigerant absorbed additional heat, increasing the suction temperature. The SAHPDs raised the chamber temperature, making them well-suited for practical applications such as herb drying. Figure 3 illustrates the actual arrangement of the SAHPD during installation.

To compare the performances of the SAHPDs to HPD, three (3) sets of tests, C1-SAHPD and C2-SAHPD- were conducted to dry 5.5 kg of pandan leaf (*Pandanus amaryllifolius*) within four (4) hours. A total of 11.545 MJ was required to dry 5.5 kg of pandan leaves in four hours. The drying system provided a minimum of 11.088 MJ at a constant temperature of 45 and a mass flow rate of 0.135 kg/s. The specific heat of pandan was calculated to be 3.39kJ/kg°C. Additionally, economic analyses were performed for each trial. The analysis results of all tests can be summarized as follows:

### HEAT PUMP DRYING MODE PERFORMANCE

During testing on January 9th, 2024, the ambient temperature (wet and dry bulb) and relative humidity were recorded at 26°C (wB), 31°C (dB), and 67%, respectively. Figure 4 illustrates the relationship between suction superheat (SSH), subcooling (SC), and the coefficient of performance (COP). The COP ranged from 5.01 to 5.77,

with the maximum COP of 5.77 achieved at SSH 15.95K and SC 9.51K. Figure 5 shows the HPD's COP and the temperature in the drying chamber. The chamber temperature increased from 28.4°C to 47°C, while the relative humidity decreased from 88.1 to 27.8. A total of 5.5 kilograms of fresh pandan leaves were dried over 4.0 hours, resulting in a final mass of 2.11 kg and a moisture extraction rate (MER) of 0.23 kg/hour. The specific moisture extraction rate (SMER) for the HPD mode was 2.64 kg/kWh. The HPD used in this experiment required approximately 6.64 kW of electricity. The energy cost to dry 5.5 kg of pandan (*Pandanus amaryllifolius*) over four hours was calculated to be 0.62 USD/kWh. Over the 20 days and eight hours of operation, the system consumed 265.6 kWh of energy to produce 84.4 kilograms of dried pandan leaves. Based on these figures, the monthly electricity cost was 32.18 USD or 0.38 USD/ kilogram of Pandan leaves.

### SOLAR-ASSISTED HEAT PUMP DRYING PERFORMANCE OF C1-SAHPD AND C2-SAHPD

Figure 6 illustrates the daily solar radiation profile, hot water, and water tank temperature at the testing site. Daily average radiation intensity exceeding 500 W/m<sup>2</sup> is suitable for running the SAHPD, compared to a minimum daily average of 430 W/m<sup>2</sup> (Qiu et al. 2016). Table 4 presents the solar energy drying system's daily average collector efficiency and heat efficiency on a typical day at UKM, Bandar Baru Bangi. Daily total radiation ranged from 14.3 MJ/m<sup>2</sup> to 15.79 MJ/m<sup>2</sup>, with the SAHPD's average energy storage efficiency ranging from 62.59% to 63.97% and heat supply efficiency from 43.29% to 51.37%. The solar fraction for C1-SAHPD and C2-SAHPD was 0.34 and 0.45, respectively. The tank's water temperature gradually increased from 28°C to 70°C. For testing, an auxiliary heater is required to raise the hot water temperature to 90°C (the tank's maximum temperature). Compared to another experiment where water was heated in a triangular-shaped

collector under the sun, the water temperature ascends to 46.6, 37.25, and 33.5°C for 4l, 14l, and 33l at roughly 5 p.m. The average storage temperature for case (1) is 49°C, higher than in the other cases(Ahmed, 2020).

**C1-SAHPD: REFRIGERANT HEATING AT DISCHARGE LINE PERFORMANCE**

Figure 7 shows that adding 90°C hot water to the discharge pipe (C1-SAHPD) resulted in notable heat absorption at high surface temperatures, especially during the first 30 minutes of testing. The discharge pipe had a surface temperature ranging from approximately 70-85°C. Subsequently, despite a positive temperature difference between hot water pipes, the refrigerant inlet temperature was higher than the outlet temperature at the HE. The refrigerant pipe inlet surface temperature at the HE remained higher than the outlet throughout the testing period. The HE effectiveness was 0.20, and the COP ranged from 5.02 to 6.20. The highest COP values were achieved at suction superheat (SSH) 16.91K and subcooling 5.88K. Figure 8 indicates that the C1-SAHPD increased COP more than HPD at the suction superheat and subcooling values. Figure 9 shows that the surface refrigerant pipe temperature inlet and outlet at the HE influenced the average temperature in the drying chamber, which increased to 44.9°C, and relative humidity decreased from 77.3 to 25.1%. The chamber temperature was consistent with the

HPD. Meunier et al. suggested adjusting the hot water supply temperature at 100, 130, and 160°C intervals for a better result.

**C2-SAHPD: REFRIGERANT HEATING BETWEEN CONDENSERS PERFORMANCE**

Figure 10 demonstrates that adding 90°C hot water between condensers (C2-SAHPD) with a low subcooled liquid surface pipe temperature of 30°C allowed for significant heat absorption during testing. The hot water temperature at 89°C gradually decreased to 69°C. Following this, there was a positive temperature difference between refrigerant pipes when the exit was higher than the inlet at the HE, with a significant gap throughout the testing period. The HE effectiveness was 0.59, and the COP ranged from 5.01 to 7.39. The highest COP values were obtained at suction superheat (SSH) 24.25K and subcooling -0.47K. Figure 11 shows that the C2-SAHPD increased COP more than the C1-SAHPD and HPD at certain suction superheat and subcooling levels. As a result, Figure 12 shows that the surface refrigerant pipe temperature inlet and outlet at the HE influenced the temperature in the drying chamber. The average chamber temperature was 51°C, higher than C1-SAHPD and HPD, with relative humidity decreasing from 66.3% to 21.5%.

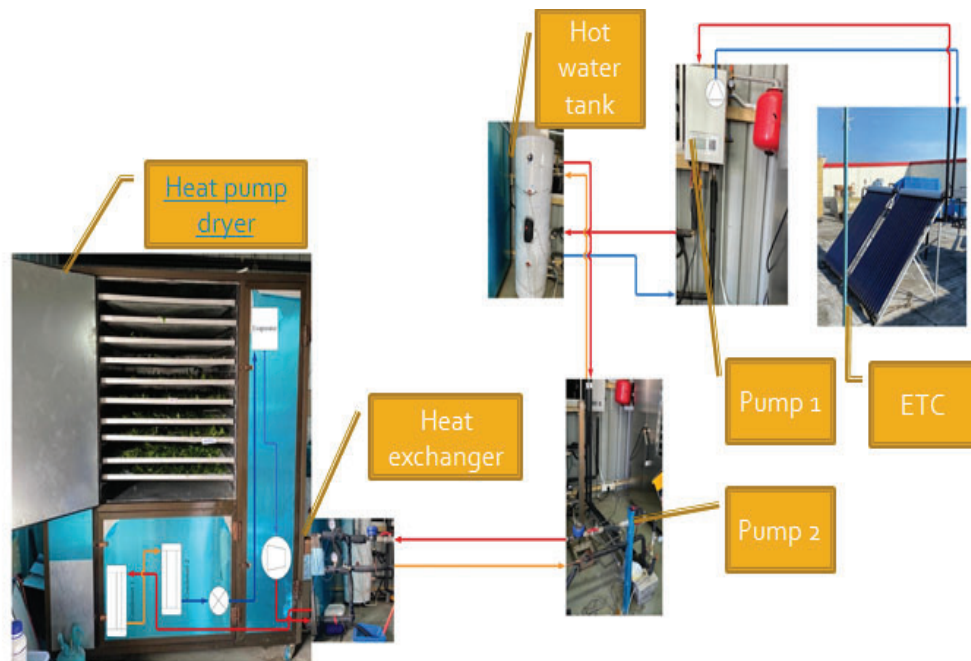


FIGURE 3. The actual arrangement of the SAHPD

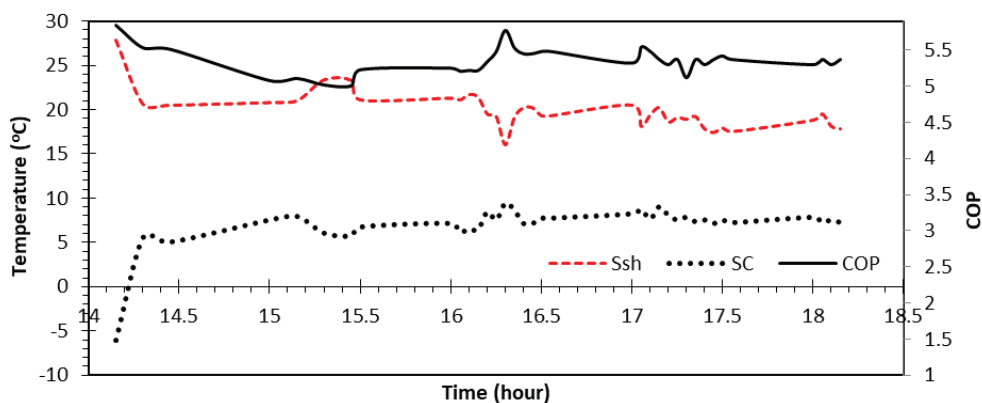


FIGURE 4. Superheat, subcooling, and COP of HPD

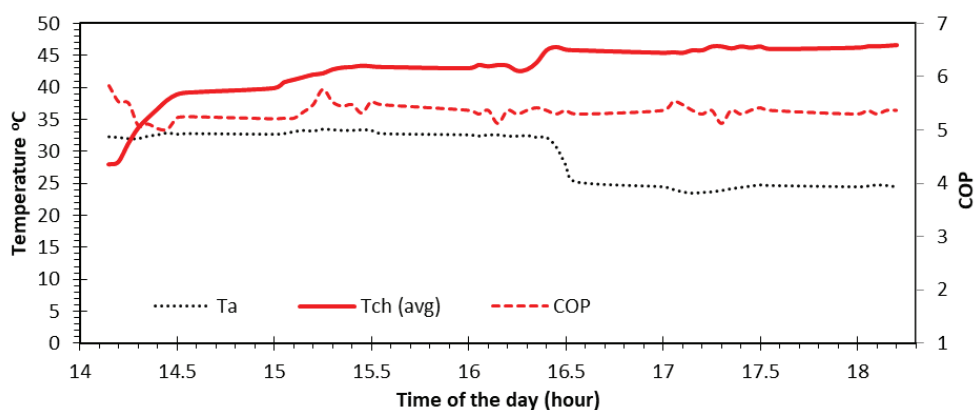


FIGURE 5. Coefficient of performance, ambient and average chamber temperature of HPD

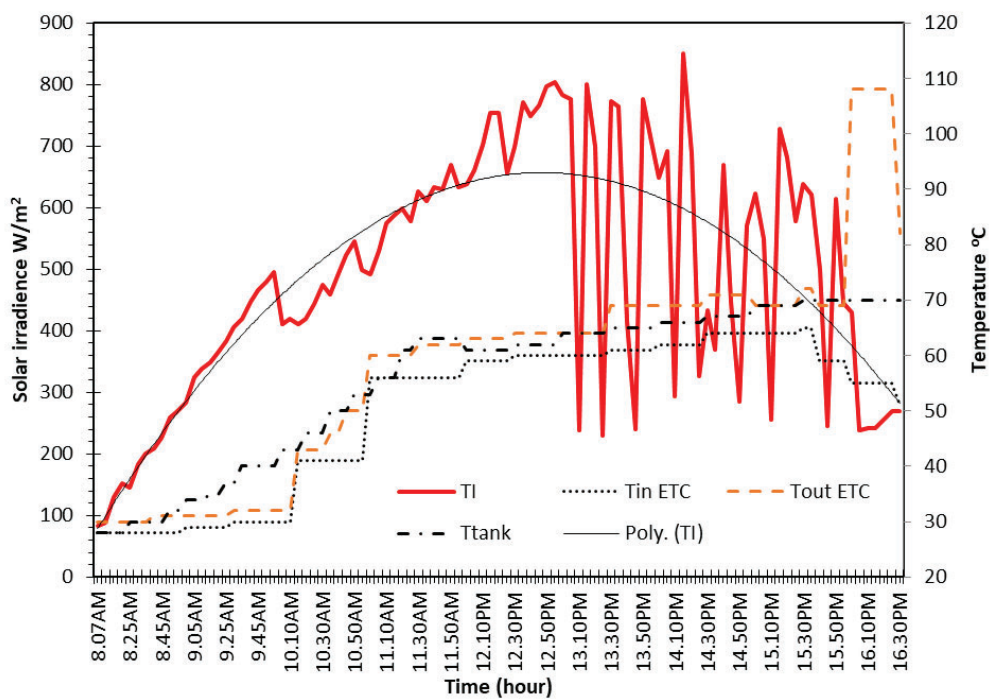


FIGURE 6. Solar irradiance (TI), hot water, and water tank temperature of SAHPDs

TABLE 4. Daily average energy storage and heat performance of SAHPDs system

Date	The Daily total radiation (MJ.m-2)	$\eta_c(\%)$	$\eta_s(\%)$	SF
Nov 15 <sup>th</sup> , 2023 C1-SAHPD	14.38	62.59	43.29	0.34
Feb 13 <sup>th</sup> , 2024 C2-SAHPD	15.65	63.97	51.37	0.45

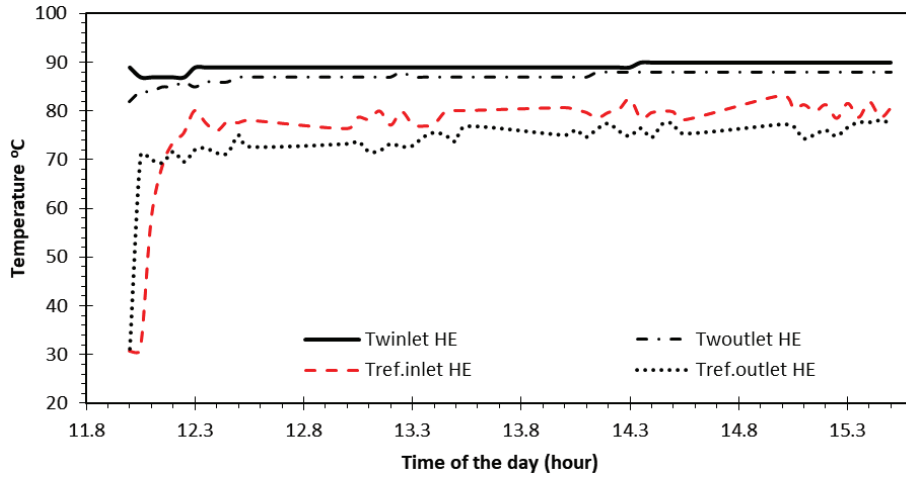


FIGURE 7. Temperature of hot water (w) and refrigerant (ref.) at the heat exchanger (HE) for C1-SAHPD

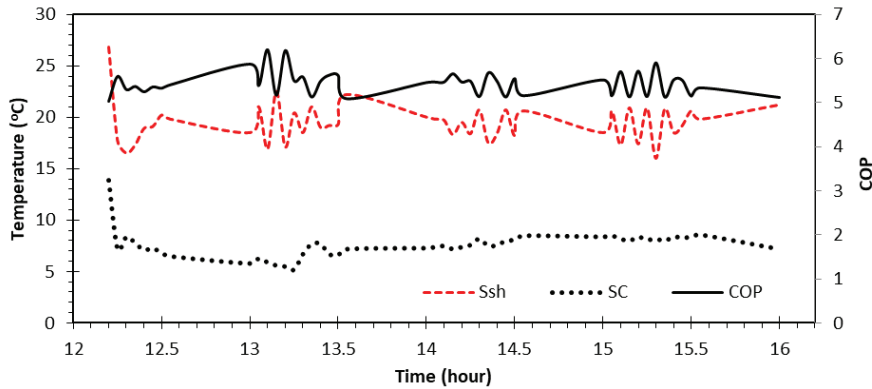


FIGURE 8. Superheat, subcooling and COP of C1-SAHPD

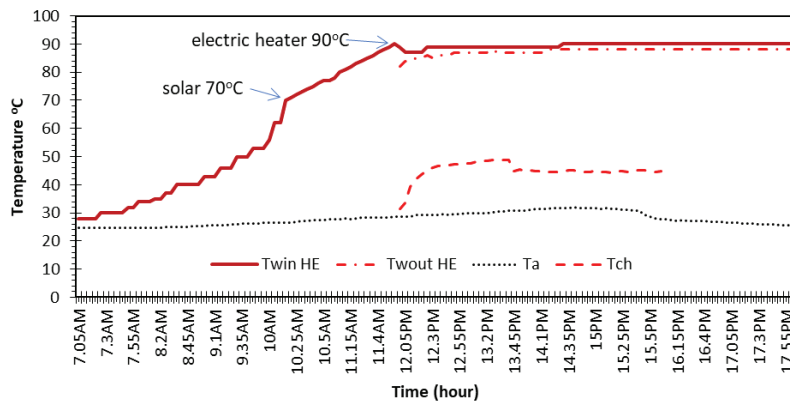


FIGURE 9. Hot water, ambient, and average chamber temperature of C1-SAHPD

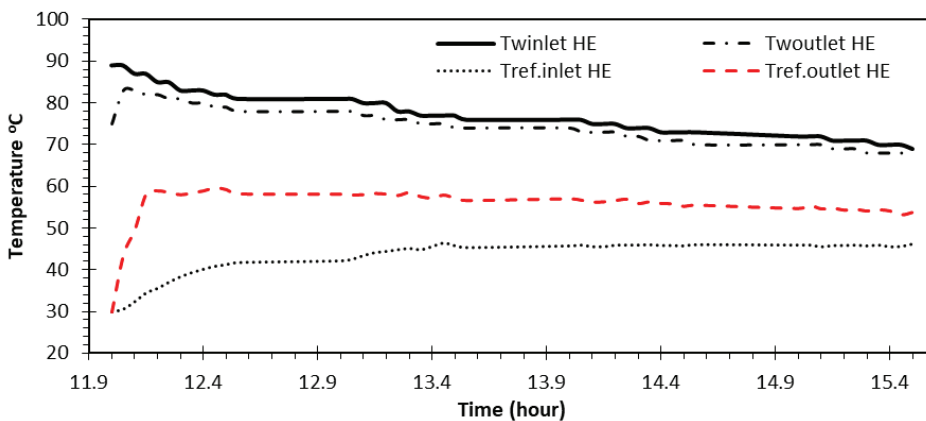


FIGURE 10. Temperature of hot water (w) and refrigerant (ref.) at the heat exchanger (HE) for C2-SAHPD

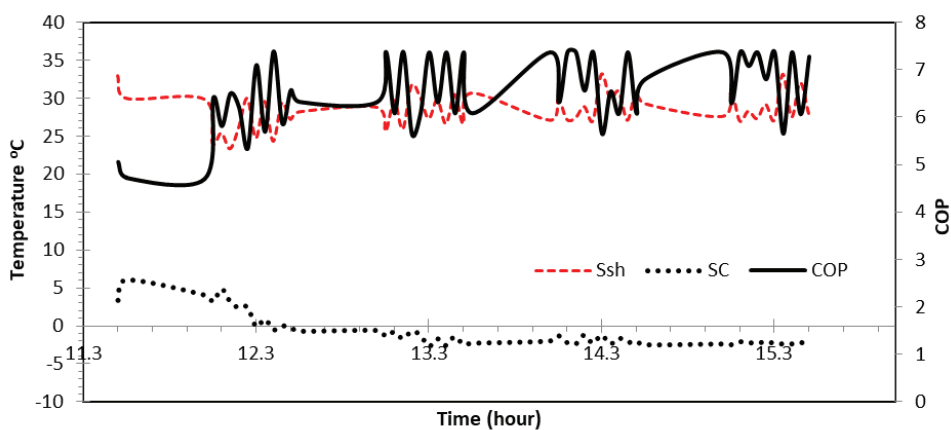


FIGURE 11. Superheat, subcooling, and COP of C2-SAHPD

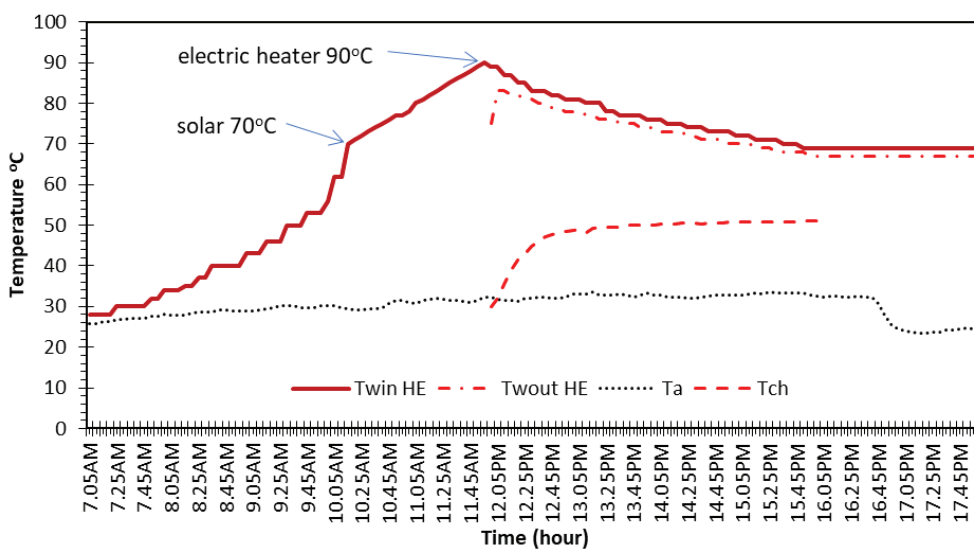


FIGURE 12. Hot water, ambient, and average chamber temperature of C2-SAHPD

## DRYING CHARACTERISTICS ANALYSIS OF PANDAN UNDER THREE EXPERIMENTS

Figure 13 presents the Mollier chart of refrigeration systems HPD, C1-SAHPD, and C2-SAHPD, generated using Solkane software. Tables 5 and 6 indicate the drying system's average coefficient of performance (COP<sub>avg</sub>): 5.34 for HPD, 5.43 for C1-SAHPD, and 6.53 for C2-SAHPD. Fresh leaves lost between 2.12 kg and 1.72 kg of their original mass in four hours or less. The specific moisture extraction rate (SMER) of HPD was 2.64. The C1-SAHPD and C2-SAHPD exhibited SMERs of 1.88 and 2.71 at solar fractions of 0.34 and 0.45, respectively.

Table 6 also provides additional performance parameters for the R-32 dryer, including the refrigerating effect: 176.03kJ/kg for HPD, 175.26kJ/kg for C1-SAHPD, and 177.00kJ/kg for C2-SAHPD. The compressor's power requirements were 1.04 kW for HPD, 0.99 kW for C1-SAHPD, and 0.72 kW for C2-SAHPD. Figure 14 illustrates the drying temperatures and relative humidity (%RH) of HPD, C1-SAHPD, and C2-SAHPD. The air output temperature of C2-SAHPD was 52.7°C with an average chamber temperature of 51°C and 21% RH, outperforming HPD (45°C, 27.5% RH) and C1-SAHPD (44°C, 24.5% RH). The air output temperature of 52.7°C surpasses that achieved by a double-pass photovoltaic/thermal solar air collector using bifacial PV with CPC and mirror reflector, which was 51°C (Saber et al. 2023). Figure 15 shows that C2-SAHPD achieved the highest COP compared to C1-SAHPD and HPD during the four-hour testing period.

Table 7 compares the coefficient of performance of the SAHPD using solar-heating air reported by E.L.Rulazi et al. Salehi et al. Hasibuan et al. and Gu et al. which were 3.25, 3.4, 4.35, and 5.03, respectively. All previous SAHPDs utilized air-heated methods with solar heating. Using solar-heating refrigerant, the current study achieved higher SMER and COP values of 2.71 and 6.53, respectively, indicating the potential for drying various types of solid material.

## ECONOMIC ANALYSIS

The cost of dried goods varies according to the drying technique used. Open-sun drying is the most cost-effective method compared to HPD and SAHPD. Table 8 shows the

cost and economic characteristics. The selling price of sun-dried pandan leaves is 25.86 USD/kg. It is assumed that the selling price of the product produced by the various drying processes differs by 20%. The study found that the HPD and SAHPD systems could be used year-round and in any location, with the yearly net present worth calculation based on 240 operational days per year.

Table 8 also reveals that employing SAHPDs increased material and personnel expenses by up to 87.50% compared to HPD. The electricity cost per weight of fresh pandan via HPD was 0.113 USD/kg, and using C1-SAHPD and C2-SAHPD lowered it by 3.5% and 46%, respectively. The power cost of the C1-SAHPD in this study is approximately 0.56 USD/kWh, similar to the PV system of DC vapour compression; however, the C2-SAHPD consumed 41% less energy (Jarimi et al. 2024). Despite large cost savings, a high-efficiency system or wise electricity usage will reduce carbon emissions, boost economic development, and be less harmful to the environment, as the correlation between energy consumption and carbon emissions is highly positive (Rajamoorthy, Bee Chen, & Munusamy, 2018), (Eng Sing et al. 2022). The annual savings or income for HPD, C1-SAHPD, and C2-SAHPD were 31,576.80 USD, 45,806.40 USD, and 51,242.40 USD, respectively. Thus, combining a heat pump drier and solar energy creates an economically viable method for drying herbs (Rulazi, Marwa, Kichonge, & Kivevele, 2024). The overall annual amount of fresh pandan in the system is 2640 kg, based on the number of leaves used during testing. Table 9 shows the calculated yearly and cumulative net present worth for Pandan's system life using the three dryer processes. For 15 years, the cumulative net present worth for HPD, C1-SAPHD, and C2-SAHPD was 299526.19 USD, 434503.06 USD, and 486067.01 USD, respectively. Based on the life cycle cost analysis (LCCA) for equipment, energy, and dryer maintenance, a domestic air-to-air heat pump (HP) has a projected service life of 15 years, with an annual maintenance cost of 7% of the system's total cost (Kirk & Dell'Isola, 1995). Drying pandan resulted in payback periods of 4.56, 4.32, and 3.84 months for the HPD, C1-SAPHD, and C2-SAHPD, respectively. Figure 16 shows the economic analysis values, indicating differences between HPD, C1-SAHPD, and C2-SAHPD. Consequently, regarding cost recovery, the C2-SAHPD dryer system was the best option for drying pandan leaves.

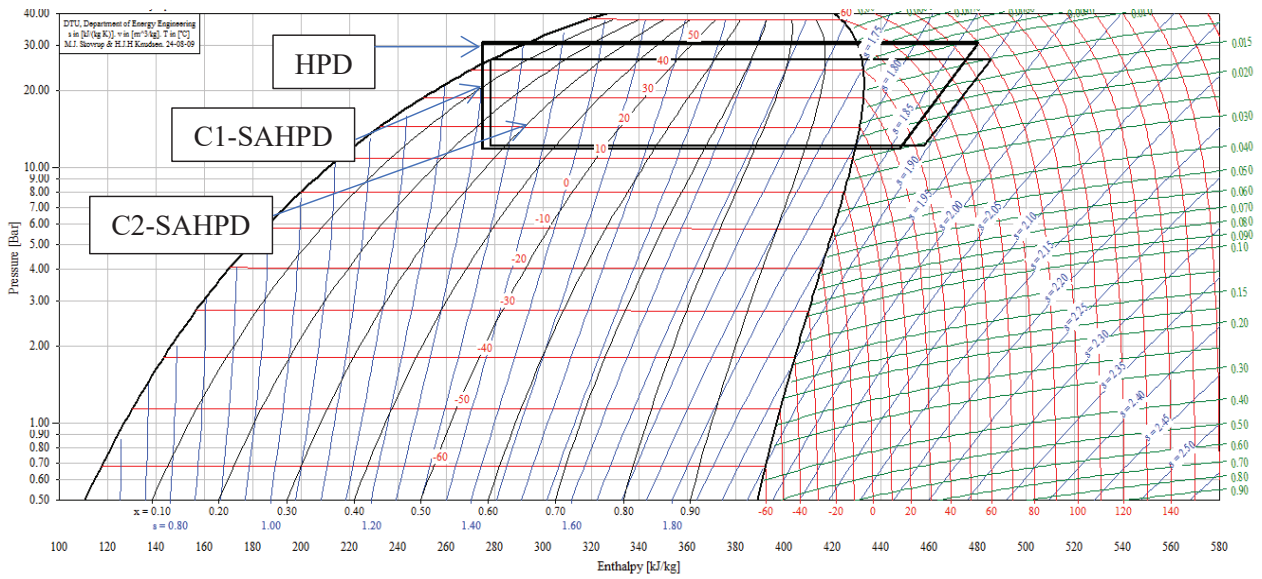


FIGURE 13. P-H diagram of HPD, C1-SAHPD and C2-SAHPD

TABLE 5. Results of drying systems from three distinct studies.

Measurement	HPD	C1-SAHPD	C2-SAHPD
SMER (kg/kW h)	2.64	1.88	2.71
COP (average)	5.34	5.43	6.53
Time (h)	4	4	4
The efficiency of energy storage	N/A	62.59	63.97
The efficiency of supplying heat	N/A	29.79	41.18
The effectiveness of HE	N/A	0.20	0.59
Solar fraction	N/A	0.34	0.45
Initial and final moisture content (g water/g dry matter)	5.4-0.34	5.4-0.34	5.4-0.34

TABLE 6. Performance of the dryer using R-32

Calculated Result	HPD	C1-SAHPD	C2-SAHPD
Refrigeration effect (kJ/kg)	176.03	175.26	177.00
Heat rejection (kJ/kg)	211.09	208.64	201.48
Refrigerant circulation rate (kg/s)	0.0199	0.0200	0.0198
Power required by compressor (kW)	1.04	0.99	0.72
Coefficient of performance (COP <sub>avg</sub> )	5.34	5.43	6.53
Compressor power per kW	0.173	0.165	0.12

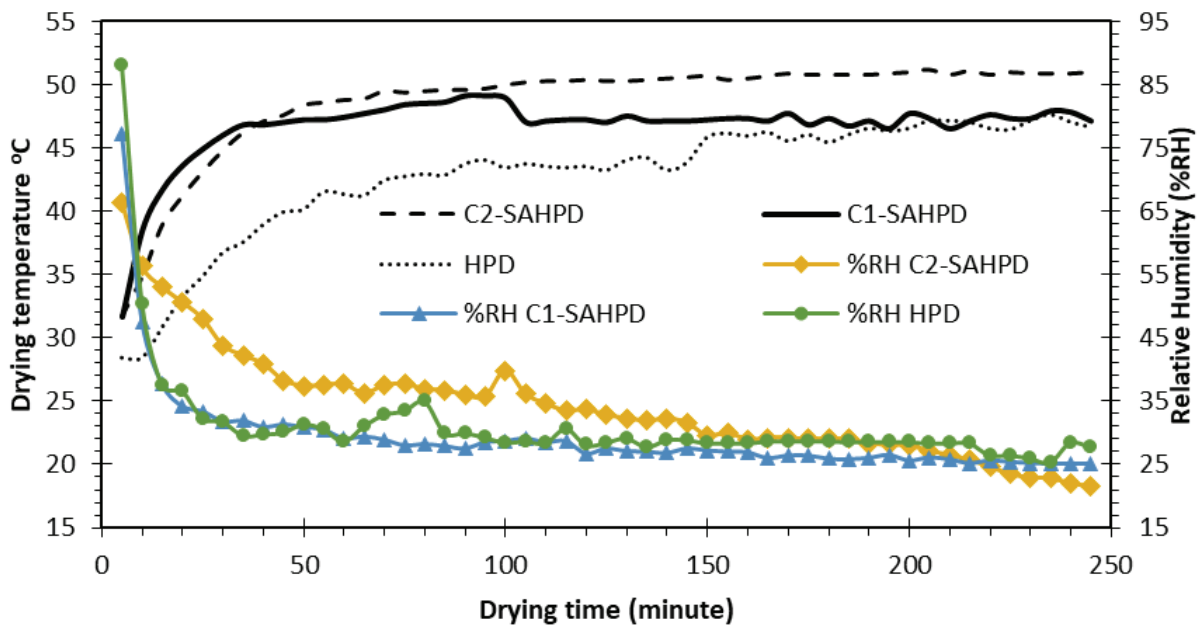


FIGURE 14. Chamber temperature and relative humidity (%RH) of HPD, C1-SAHPD, and C2-SAHPD

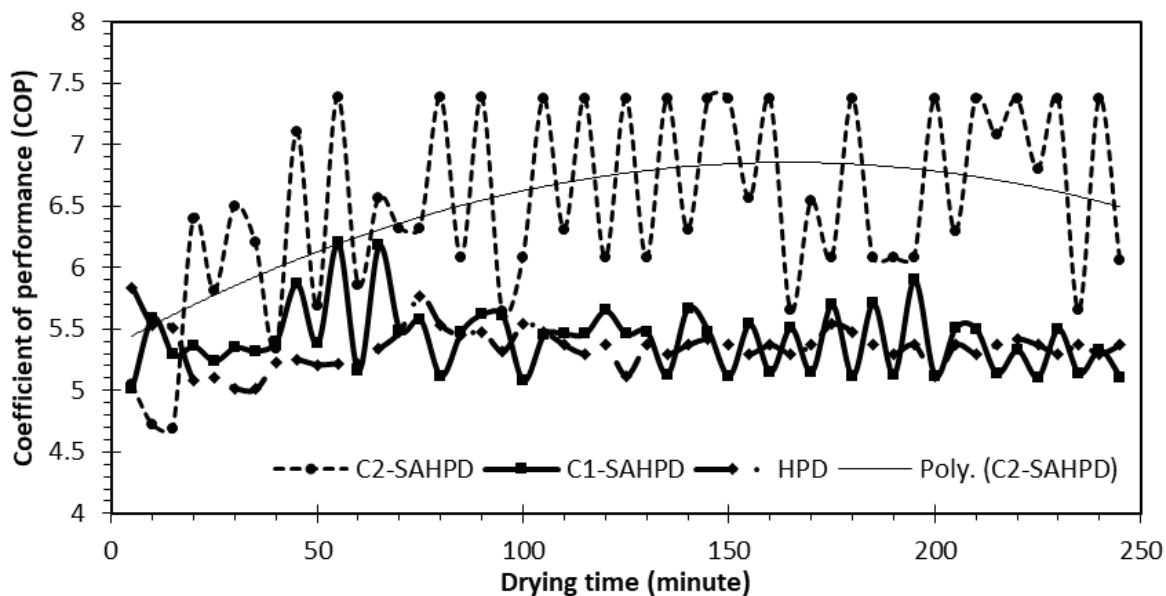


FIGURE 15. Coefficient of performance (COP) of HPD, C1-SAHPD, and C2-SAHPD

TABLE 7. Comparison of previous work with current work

Dryer type	Material dried	Load (kg)	Drying time (h)	Drying temp. (°C)	SMER (kg/kWh)	COP Reference
SAHPD	Curcuma	30.5	8	57.7	2.07	4.35 Hasibuan et al. (2020)
SAHPD	Pineapples	0.6	5	43	0.26	3.25 Salehi et al. (2021)
SAHPD	Banana	2.5	8	32	0.45	5.34 (Candan, Oktay, & Coskun, 2021)
SAHPD	Grain	3760	42	41.8	1.934	5.03 Gu et al. (2022)
SAHPD	Tomato	30	12	45-65	1.33	3.4 E.L.Rulazi et al. (2023)

continue ...

... cont.

SAHPD	Paddy	420	5.5	62.9	0.44	3.26 (Yahya, Fahmi, Hasibuan, & Fudholi, 2023)
SAHPD	Tobacco leaf	15	10	66	1.30	3.4 (Suleiman, Pogrebnoi, & Kivevele, 2023)
SAHPD	Banana	0.5	4.5	48.71	0.13	3.69 (Loemba, Kichonge, & Kivevele, 2024)
SAHPD	Pandan leaf	5.5	4	51	2.71	6.53 current work

TABLE 8. Cost and economic parameters.

ITEM	HPD	C1-SAHPD	C2-SAHPD
Material and labor cost (USD)	4310.34	8081.89	8081.89
Annually, product cost	5702.40	5702.40	5702.40
Annually energy cost	57.75	82.84	63.00
Annually saving	31,576.80	45,806.40	51,242.40
Inflation rate	4%	4%	4%
Interest of long term investment rate	10%	10%	10%
Life period of the dryer (years)	15	15	15
Price of fresh Pandan (Shopee,2024),USD/kg	2.16	2.16	2.16
Selling price of dried Pandan (Shopee,2024)	31.03	37.24	37.24
Electricity cost (USD/kWh)	0.62	0.60	0.33
Electricity cost (USD/kg)	0.113	0.109	0.061

TABLE 9. Economic of dried pandan for HPD, C1-SAHPD and C2-SAHPD.

Year	HPD		C1-SAHPD		C2-SAHPD	
	Annual net present worth	Cumulative net present worth	Annual net present worth	Cumulative net present worth	Annual net present worth	Cumulative net present worth
1	28706.18	28706.18	41642.18	41642.18	46584.00	46584.00
2	27140.26	55846.44	39370.60	81012.78	44042.84	90626.84
3	25659.31	81505.75	37222.28	118235.06	41639.57	132266.42
4	24260.46	105766.20	35193.06	153428.12	39369.54	171635.95
5	22937.39	128703.59	33273.77	186701.89	37222.48	208858.43
6	21686.00	150389.59	31458.46	218160.35	35191.74	244050.18
7	20503.13	170892.72	29742.55	247902.90	33272.20	277322.38
8	19384.68	190277.40	28120.09	276023.00	31457.20	308779.58
9	18327.49	208604.90	26586.49	302609.49	29741.60	338521.18
10	17327.77	225932.66	25136.26	327745.75	28119.27	366640.44
11	16382.68	242315.34	23765.28	351511.03	26585.58	393226.03
12	15631.15	257946.49	22675.08	374186.11	25366.01	418592.04
13	14644.06	272590.54	21243.18	395429.29	23764.18	442356.21
14	13845.48	286436.02	20084.73	415514.02	22468.26	464824.47
15	13090.16	299526.19	18989.04	434503.06	21242.54	486067.01

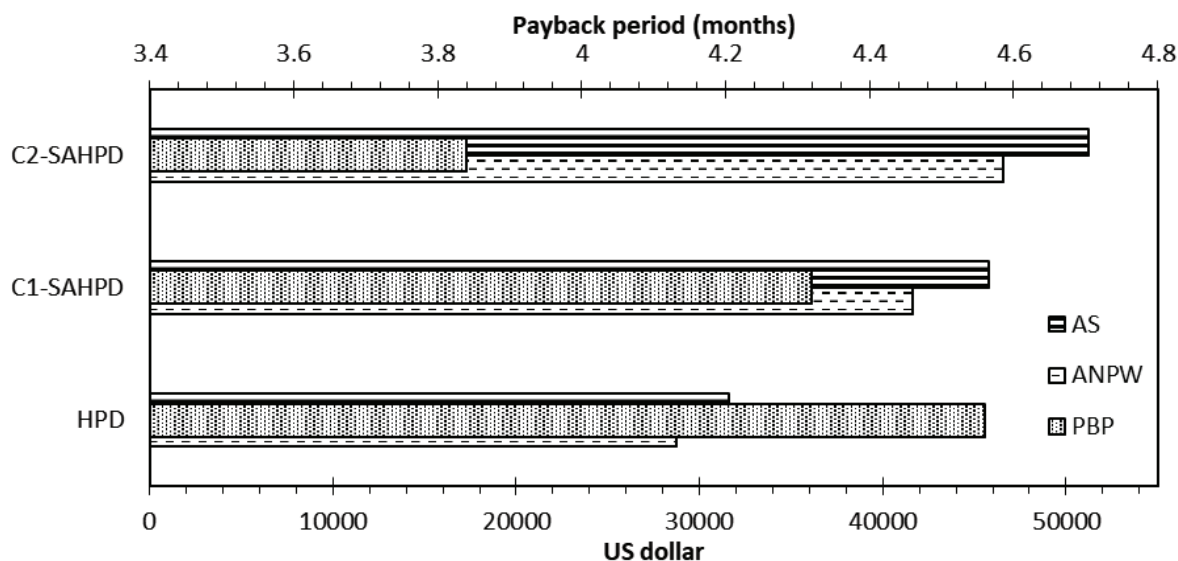


FIGURE 16. Annual saving (AS), annual net present worth (ANPW), and payback period (PBP) of HPD, C1-SAHPD, and C2-SAHPD

## CONCLUSION

This study's proposed novel solar-assisted heat pump drying system for herbs demonstrates the potential for improved efficiency, increased drying temperature, and enhanced sustainability. The total heat required for drying 5.5 kg of pandan leaf (*Pandanus amaryllifolius*) is 11.545 MJ. Analysis results for the three setups: HPD without solar, SAHPD configuration 1 (C1-SAHPD) with solar-heated refrigerant at the discharge line, and SAHPD configuration 2 (C2-SAHPD) with solar-heated refrigerant between condensers, along with their economic analyses, were conducted. All three testing configurations used identical parameters: 5.5 kg product mass, 0.135 kg/s air flow rate, and refrigerant charge at 9.65 bar. The SAHPDs operated when the daily average radiation intensity ranged from 0.670 to 1.102 kW/m<sup>2</sup> and the hot water temperature was 90°C. The research conclusions are as follows:

1. The study found that the drying system's average coefficient of performance ( $COP_{avg}$ ) to be 5.34, 5.43, and 6.53 for HPD, C1-SAHPD, and C2-SAHPD, respectively. Additionally, C1-SAHPD and C2-SAHPD reduced electricity consumption by 3.5% and 46%, respectively, compared to HPD. C2-SAHPD also improved HE efficacy from 0.20 to 0.59. Making C2-SAHPD the recommended configuration for its highest coefficient of performance (COP) and lowest electricity consumption.
2. The study also determined that employing C2-SAHPD, ideal for herb drying applications, increased the average temperature of the drying chamber from 45°C to 51 °C while decreasing relative humidity from 27% to 21%. The specific moisture extraction rate (SMER) of HPD was 2.64, while C1-SAHPD and C2-SAHPD exhibited SMERs of 1.88 and 2.71 at the solar fractions 0.34 and 0.45, respectively.
3. Economic analysis revealed that when the price of dried product increased by 20% of the price of dried pandan leaf by using sun drying, C1-SAHPD and C2-SAHPD reduced drying time by 20 and 40%, and reduced electricity costs by 3.5% and 46%, respectively, resulting in annual saving or income increases of 31,576.80 USD, 45,806.40 USD, and 51,242.40 USD, respectively. Consequently, the cumulative net present worth for 15 years was 299,526.19 USD, 434,503.06 USD, and 486,067.01 USD for the HPD, C1-SAPHD, and C2-SAHPD, respectively.
4. According to life cycle cost analysis (LCCA), the payback period for drying 11 kg of pandan leaves per day was 4.56, 4.32, and 3.84 months for HPD, C1-SAPHD, and C2-SAHPD, respectively. As a result, the study concluded that C2-SAHPD was the best dryer system for drying pandan leaves in terms of efficiency, SMER, and cost recovery. Furthermore, this study's performance optimization helped develop a new technique for classifying dryer technologies.

## CREDIT AUTHORSHIP CONTRIBUTION STATEMENT

Rohaimi Abdullah: writing – review & editing, writing – original draft, validation, methodology, investigation, data curation, conceptualization. Adnan Ibrahim: writing - review & editing, validation, supervision, project administration, funding acquisition, and conceptualization. Muhammad Amir Aziat Bin Ishak – writing – review & editing, validation, supervision, methodology, data curation. Kamaruzzaman Sopian: writing - review & editing, validation, supervision, methodology, data curation. Hasila Jarimi: writing - review & editing, validation, supervision, methodology, data curation. Halim Razali: writing – review & editing, validation, supervision, methodology, data curation. Ghaith Abusaibaa: writing – original draft, validation, resources, methodology, investigation, data curation.

## ACKNOWLEDGEMENT

Sincerely thank the Solar Thermal and Sustainable Technology Group, under Sustainable Resources, Nature and Smart Living Cluster, Kumpulan Penyelidikan Universiti (KPU), and Institut Penyelidikan Tenaga Suria, Universiti Kebangsaan Malaysia, for their invaluable support and guidance throughout this project.

## DECLARATION OF COMPETING INTEREST

The authors declare that they have no known competing financial interests or personal relationships that could have appeared to influence the work reported in this paper.

enhancement of nanofluids spray in shell and tube heat exchanger. *Energy Conversion and Management* 8(2): 324–346. <https://doi.org/10.25156/ptj.2018.8.2.206>

Abusaibaa, G., Sopian, K., Abdullah, R., Jarimi, H., & Ibrahim, A. 2022. Performance analysis of solar assisted heat pump drying system with dual condensers. *Journal of Advanced Research in Fluid Mechanics and Thermal Sciences* 99(1): 134–148. <https://doi.org/10.37934/arfmts.99.1.134148>

Ahmed, O. K. 2020. *Performance Assessment of a Triangular Integrated Collector Using Neural Networks*. 10(1): 175–181.

- Ardita, I. N., Wirajati, I. G. A. B., & Sudirman. 2020. The effect of changing superheat degrees on energy consumption in a split air conditioning. *Journal of Physics: Conference Series* 1450(1). <https://doi.org/10.1088/1742-6596/1450/1/012091>
- Assadeg, J., Alwaeli, A. H. A., Sopian, K., Moria, H., Hamid, A. S. A., & Fudholi, A. 2020. Solar assisted heat pump system for high quality drying applications: A critical review. *International Journal of Renewable Energy Research* 10(1): 303–316. <https://doi.org/10.20508/ijrer.v10i1.10403.g7876>
- Boroze, T., Desmorieux, H., Méot, J. M., Marouze, C., Azouma, Y., & Napo, K. 2014. Inventory and comparative characteristics of dryers used in the sub-Saharan zone: Criteria influencing dryer choice. *Renewable and Sustainable Energy Reviews* 40: 1240–1259. <https://doi.org/10.1016/j.rser.2014.07.058>
- Candan, D., Oktay, Z., & Coskun, C. 2021. Design and an instantaneous experimental analysis of photovoltaic-assisted heat pump dryer for agricultural applications using banana chips. *Journal of Food Process Engineering*, 44(10): 1–25. <https://doi.org/10.1111/jfpe.13832>
- Chen, W. L., Wong, K. L., & Li, Y. C. 2015. Innovative dual storage heat tank combination solar thermal, air conditioners and heat pump of water heating systems. *Sains Malaysiana* 44(12): 1707–1714.
- Daghigh, R., Ruslan, M. H., Sulaiman, M. Y., & Sopian, K. 2010. Review of solar assisted heat pump drying systems for agricultural and marine products. *Renewable and Sustainable Energy Reviews* 14. <https://doi.org/10.1016/j.rser.2010.04.004>
- Din, S. I. U., Ibrahim, A., Ajeel, R. K., Fazlizan, A., Ishak, A. A., & Al-Aasam, A. B. 2024. Thermal performance analysis of a double-pass solar air heater with lava rock as porous and sensible heat storage material. *Journal of Energy Storage* 95(June): 112564. <https://doi.org/10.1016/j.est.2024.112564>
- Eng Sing, T., Mustafa, M. S. S., Zakaria, A. F., Mohamed Yusop, F., Saji, N., Abdul Rahman, M. F., & Sari, K. A. 2022. Study on energy efficiency using Building Information Modelling (BIM) at shared library Pagoh Higher Education Hub. *Jurnal Kejuruteraan* si5(2): 3–8. [https://doi.org/10.17576/jkukm-2022-si5\(2\)-01](https://doi.org/10.17576/jkukm-2022-si5(2)-01)
- Hawllader, M. N. A., & Jahangeer, K. A. 2006. Solar heat pump drying and water heating in the tropics. *Solar Energy* 80: 492–499.
- Jarimi, H., Zheng, T., Zhang, Y., Razak, T. R., Ahmad, E. Z., Wan Roshdan, W. N. A., ... Riffat, S. 2024. Solar photovoltaic-assisted DC vapour compression with a low-cost ice gel thermal battery for off-grid building cooling. *Journal of Building Engineering* 91(January): 109350. <https://doi.org/10.1016/j.job.2024.109350>

- Kareem, B. E., & AlHayes, R. A. M. 2018. Experimental and theoretical study of dew point evaporative cooling system suitable for erbil climate. *Polytechnic Journal* 8(2). <https://doi.org/10.59341/2707-7799.1787>
- Khouya, A. 2020. Performance assessment of a heat pump and a concentrated photovoltaic thermal system during the wood drying process. *Applied Thermal Engineering* 180: 115923. <https://doi.org/10.1016/j.applthermaleng.2020.115923>
- Kirk, S. J. & Dell'Isola, A. J. 1995. Life cycle costing for design professionals. In *Proceedings of Joint International Symposium of CIB Working Commissions W55/W65/W107 in Knowledge Construction*.
- Loemba, A. B. T., Kichonge, B., & Kivevele, T. 2024. Thermal performance and technoeconomic analysis of solar-assisted heat pump dryer integrated with energy storage materials for drying cavendish banana (*musa acuminata*). *Journal of Food Processing and Preservation* 2024. <https://doi.org/10.1155/2024/7496826>
- Meunier, F., Rivet, P., T. 2005. *Froid Industriel*. Dunod, Paris.
- Meunier Francis, D. M. 2013. *La Climatisation Solaire*.
- Murtini, E. S., Yuwono, S. S., Setyawan, H. Y., & Nadzifah, N. 2020. Pandan leaf powder: Characteristics and its application in Pandan sponge cake making. *IOP Conference Series: Earth and Environmental Science* 475(1). <https://doi.org/10.1088/1755-1315/475/1/012041>
- Ochs, F., Magni, M., & Dermentzis, G. 2022. Integration of heat pumps in buildings and district heating systems—Evaluation on a building and energy system level. *Energies* 15(11). <https://doi.org/10.3390/en15113889>
- Qiu, Y., Li, M., Hassanién, R. H. E., Wang, Y., Luo, X., & Yu, Q. 2016. Performance and operation mode analysis of a heat recovery and thermal storage solar-assisted heat pump drying system. *Solar Energy* 137: 225–235. <https://doi.org/10.1016/j.solener.2016.08.016>
- Rajamoorthy, Y., Bee Chen, O., & Munusamy, S. 2018. Evidence of electricity consumption lead climate change in Malaysia. *Jurnal Kejuruteraan* si1(6): 49–58. [https://doi.org/10.17576/jkukm-2018-si1\(6\)-07](https://doi.org/10.17576/jkukm-2018-si1(6)-07)
- Reddy, T. A. 2008. Active solar heating systems. In *Energy Conversion* (pp. 18–1).
- Rulazi, E. L., Marwa, J., Kichonge, B., & Kivevele, T. T. 2024. Techno-economic analysis of a solar-assisted heat pump dryer for drying agricultural products. *Food Science and Nutrition* 12(2): 952–970. <https://doi.org/10.1002/fsn3.3810>
- Saberi, Z., Jarimi, H., Hj Jumali, M. H., Suhendri, S., Riffat, S., Fudholi, A., ... Sopian, K. 2023. Performance assessment of double pass photovoltaic/thermal solar air collector using bifacial PV with CPC and mirror reflector under Malaysian climate. *Case Studies in Thermal Engineering* 44(February): 102811. <https://doi.org/10.1016/j.csite.2023.102811>
- Singh, P., & Gaur, M. K. (2020). Review on development, recent advancement and applications of various types of solar dryers. *Energy Sources, Part A: Recovery, Utilization, and Environmental Effects* 0(0): 1–21. <https://doi.org/10.1080/15567036.2020.1806951>
- Suleiman, S. A., Pogrebnoi, A., & Kivevele, T. T. 2023. Influence of Duct Configurations on the Performance of Solar-Assisted Heat Pump Dryer for Drying Tobacco Leaves. *International Journal of Photoenergy* 2023. <https://doi.org/10.1155/2023/4588407>
- Yahya, M., Fahmi, H., Hasibuan, R., & Fudholi, A. 2023. Development of hybrid solar-assisted heat pump dryer for drying paddy. *Case Studies in Thermal Engineering* 45(January): 102936. <https://doi.org/10.1016/j.csite.2023.102936>
- Yang, Z., Zhu, Z., & Zhu, E. 2013. Experimental research on parallel conversion control of drying temperature in a closed-loop heat pump dryer. *Drying Technology* 31(9): 1049–1055. <https://doi.org/10.1080/07373937.2013.772898>
- Zou, L., Liu, Y., Yu, M., & Yu, J. 2023. A review of solar assisted heat pump technology for drying applications. *Energy* 283: 129215. <https://doi.org/10.1016/j.energy.2023.129215>